Sculpted substrates for SERS

Suzanne Cintra,[a] Mamdouh E. Abdelsalam,[a] Philip N. Bartlett,*[a] Jeremy J. Baumberg,*[b] Timothy A. Kelf,[b] Yoshihiro Sugawara[b] and Andrea E. Russell*[a]

Received 22nd June 2005, Accepted 26th July 2005
First published as an Advance Article on the web
DOI: 10.1039/b508847j

Sculpted SERS-active substrates are prepared by assembling a closed packed monolayer of uniform polystyrene colloidal particles (diameter 350 to 800 nm) onto an evaporated gold surface and then electrodepositing gold through this template to produce films with controlled thicknesses, measured as fractions of the sphere diameter, *d*. The resulting surfaces consist of a regular hexagonal array of interconnected spherical cross-section dishes. The role of localised plasmons in determining the SERS enhancement factor obtained for benzene thiol adsorbed onto the surfaces is then investigated by correlation of the UV-visible reflectance spectra, 400 to 900 nm, measured at the same positions on the substrate surfaces, with the SERS spectra. The results are interpreted in terms of the relative contributions of plasmons that are free to propagate across the top surface and those trapped within the dishes of the sculpted surface.

Introduction

Surface Enhanced Raman Spectroscopy (SERS) was first observed in Southampton by Fleishmann and coworkers[1] over 30 years ago. In their experiment they found Raman spectra for pyridine adsorbed on a roughened silver electrode that were a million fold more intense than anything previously seen. At first this increase in signal was attributed to the increased surface area of the roughened silver electrode over a smooth electrode. However, it was later recognised by Jeanmarie and Van Duyne[2] and by Albrecht and Creighton[3] that the roughness could only account for a factor of 10 increase in the signal and that the true origins of the enhancement were related to the strength of the local electromagnetic field. Since this discovery the mechanism by which the local electromagnetic field perturbs the spectral response of the adsorbate has been the subject of intensive debate. It is now generally accepted that there are two contributions to the surface enhancement;[4] a charge transfer enhancement[5] (CT) arising from chemisorption of the adsorbate at the metal surface and an electromagnetic enhancement[6] (EM). Of these two mechanisms, the EM enhancement is usually the more significant and is not adsorbate specific.

The EM enhancement arises from focusing the electric field *via* plasmon resonances of the metallic substrate[7–9] at certain places on the metal surface, and is therefore strongly dependent on the surface morphology and precise shape of the roughness features at the metal surface. Recent developments in fabricating plasmonic nanostructures have enabled systematic investigations of the role of localised plasmon resonances in determining the magnitude of the EM enhancement.[10,11] Substrates have been fabricated with a variety of structures including nano-triangles[10] (by nanosphere lithography), nanorings,[12] spherical nanoshells,[13] two dimensional gratings,[14] and most recently arrays of spherical nanovoids.[15] The variety of structures enables plasmon resonant modes of differing spatial geometries to be investigated with various degrees of control over the nanostructure that is fabricated.

In the case of the spherical nanovoids to be discussed in this paper control of both the diameter of the spherical voids and their depth, or fraction of the spherical segment deposited, make such

[a] *School of Chemistry, University of Southampton, Southampton, UK, SO17 1BJ*
[b] *School of Physics and Astronomy, University of Southampton, Southampton, UK, SO17 1BJ*

structures highly tuneable. In the work presented herein the dependence of the SERS enhancement for a variety of sculpted spherical nanovoid substrates will be compared. Careful attention will be paid to the relationship between the localised plasmon resonances of the substrates, as determined by measuring the reflectance spectra, and the enhancement factors obtained.

Experimental

The sculpted substrates were formed using the templated electrodeposition process described by Bartlett *et al.*,[16,17] in which gold (or another desired metal) is electrodeposited onto a conducting surface through a template of self-assembled polystyrene latex spheres. Monodisperse solutions of the spheres were obtained from Duke Scientific as a 1 wt% aqueous suspension. The monolayer template was produced by a capillary force method that left a well-ordered hexagonal array of spheres on a gold-coated glass slide. Gold was deposited from a commercial cyanide free gold plating solution (Tech. Gold 25, Technic Inc. Cranston, RI). Following electrodeposition, the latex spheres were removed by dissolving in tetrahydrofuran, leaving an ordered array of interconnected spherical cross-section dishes. A representation of the sculpted surface formed is shown in Fig. 1.

As will be discussed in this paper, the optical properties of the sculpted substrate can be controlled by varying the diameter of the spheres and/or the thickness of the electrodeposited film. Monodisperse solutions of spheres were used with diameters, d, in the range 350 nm to 800 nm and the film heights were graded from $0d$ to $0.8d$. The thickness of the metal deposited was controlled by monitoring the charge passed during the electrodeposition. Samples were prepared with steps in thickness along the length of the gold-coated glass slide by incrementally removing the glass slide from the plating bath in steps of 500 μm.

The structure and quality of the sculpted gold films were confirmed using an environmental scanning electron microscope (Philips XL30 ESEM). Images were recorded at magnifications of up to ×20 000.

All reflectance spectra were recorded using a BX51 TRF Olympus optical microscope. The samples were illuminated by a white light source and the images were recorded using a CCD camera (DP2 Olympus). A fibre optic coupled spectrometer (Ocean Optics, spectral range 300 nm to1000 nm, resolution 1 nm) placed in the focal plane of the image was used to record the spectral response from the selected area with a spot size of 50 μm.

All Raman spectra were collected using a Renishaw Raman 2000 system with a 633 nm HeNe laser with a power of 3 mW, unless otherwise specifically stated. Spectra were collected using the extended scanning mode from 200 to 3200 $cm^{-1}$and 10 s accumulation time, with the single scan over the desired range taking 1 min to collect. A ×50 objective was used, providing a 5 μm spot at the sample.

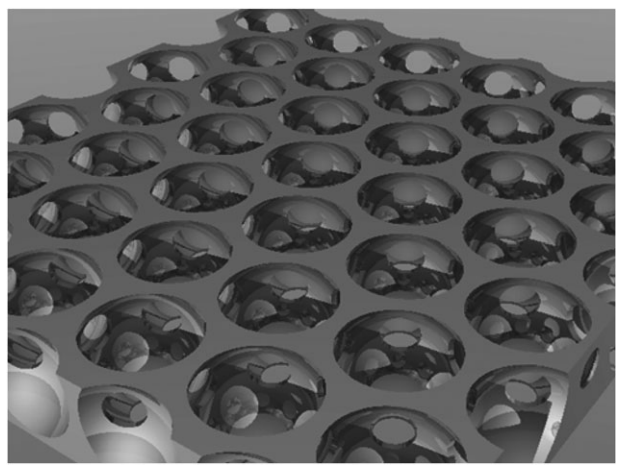

Fig. 1 Representation of a sculpted substrate grown to a thickness of 0.5 times the sphere diameter.

A 1 mmol dm^{-3} solution of benzene thiol prepared in ethanol was used as the adsorbate for all measurements. Each sample was immersed in this solution for 30 min. Excess solution was then removed by rinsing with ethanol, and the samples were left to dry in air for 15 min before the Raman measurements were taken.

The same areas of the samples were used for both Raman and reflectance spectra. Well-ordered areas of sample were pinpointed using the SEM images and the optical images were used to find irregularities and defects in the film as reference points. Replicate measurements were made to verify the spectra were a true representation of each step in film thickness.

For comparison purposes, an electrochemically roughened gold surface was also prepared using the method described by Tian *et al.*[18] Briefly, a gold-coated glass slide was placed into a 0.1 mol dm^{-3} KCl solution and the potential was swept between −0.3 V and 1.2 V *vs.* a saturated calomel reference electrode at a scan rate of 1 V s^{-1}. The potential was then held at 1.2 V for 30 s, followed by sweeping the potential back to −0.3 V at a rate of 0.5 V s^{-1}, and subsequently holding the potential at −0.3 V for 1.2 s. This procedure was repeated 25 times, yielding a roughened substrate with a dark brown coloured surface. The roughened film was rinsed well with purified water prior to use.

Results and discussion

SEM images of the electrochemically roughened and a sculpted SERS substrate, prepared using spheres with a diameter of 600 nm grown to 0.35*d*, are shown in Fig. 2 taken at the same magnification. The sculpted substrate has a very smooth surface finish in comparison to that of the electrochemically roughened surface. The roughness factor, which is the ratio of the actual surface area to the geometric surface area, of the sculpted surface was determined electrochemically by measuring the charge associated with removal of a monolayer of oxide formed on the gold surface and was found to be 1.6 for the sculpted surface shown in Fig. 2. Typical roughness factors in excess of 100 are obtained for similar measurements on electrochemically roughened gold surfaces.

The SERS spectra of benzene thiol adsorbed on both types of SERS substrates are shown in Fig. 3. As can be clearly seen, the SERS intensity obtained using the sculpted surface was significantly greater than that for the roughened surface. In addition, and in agreement with our previously reported study,[15] the SERS signal obtained using the roughened surface varied by a factor of ~ 10 (1000%) across the substrate surface, whilst the variation across the sculpted surface was 10%.

The SERS enhancement factors, EF, were calculated for both surfaces using the method described by Tian *et al.*[18] for data collected using confocal Raman spectrometers in which the surface enhancement factor (EF), *G*, is defined as follows:

$$G = \frac{c_\infty N_A \sigma h I_{\text{surf}}}{R I_{\text{bulk}}} \quad (1)$$

Thus, the intensity of the Raman peak obtained at the SERS surface, I_{surf}, is compared to that obtained for a solution, I_{bulk}, of concentration c_∞. N_A is Avogadro's number, σ is the surface area occupied by the adsorbate, *R* is the roughness factor of the surface, and *h* (units of μm) is a parameter defined by the confocal volume of the spectrometer (100 μm for the objective used in this

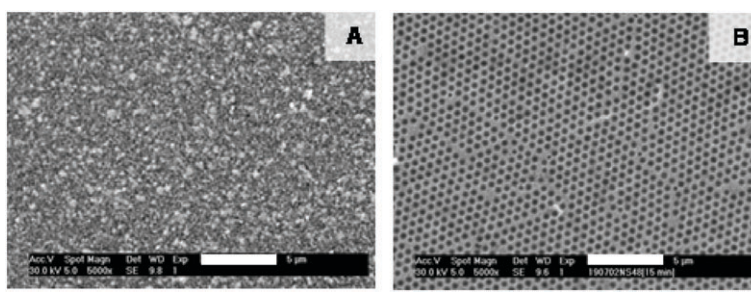

Fig. 2 SEM images of (a) an electrochemically roughened gold substrate and (b) a sculpted substrate prepared using 600 nm diameter spheres, *d*, and grown to a film height of 0.35*d*.

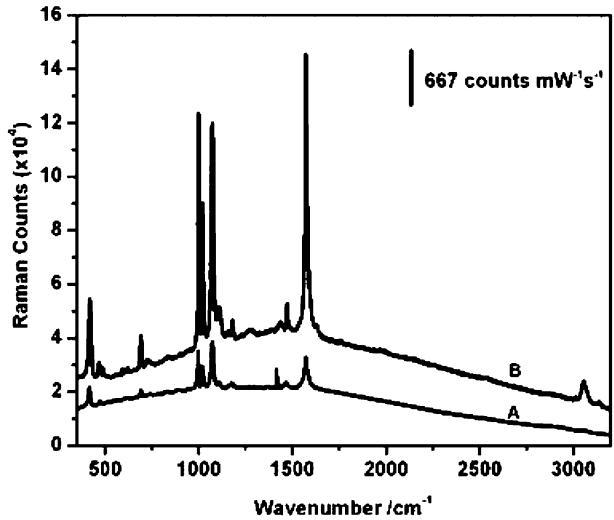

Fig. 3 SERS spectra of benzene thiol adsorbed on the substrates depicted in Fig. 2 using 633 nm excitation, 3 mW laser power at the sample, and a 10 s accumulation time.

study). EF values of 2.3×10^5 and 2.6×10^7 were obtained for the electrochemically roughened and sculpted surfaces shown in Fig. 2, respectively. The EF obtained for the sculpted surface compares favourably to the EFs in the range of 6.3×10^7 to 9.0×10^7 reported by Haynes and Van Duyne for nanosphere lithographically produced silver nanoparticles.[10] The lower value obtained for our sculpted surfaces may reflect the decreased nanoscale roughness of the electrochemically deposited films compared to those prepared using metal vapour deposition or sputtering. Such nanoscale roughness is thought to provide additional local field enhancements beyond those produced by the underlying templated nanostructure.[11] In addition, larger EFs are generally obtained for silver substrates than for gold substrates with similar structures. Indeed, we have found this to be the case for sculpted substrates prepared using the templated electrodeposition method, obtaining EFs that were up to an order of magnitude greater for the sculpted silver surfaces.[19]

An advantage of the sculpted surfaces reported here over the nanosphere lithographic method is that, in addition to varying the sphere diameter, the film height can also be varied, yielding a greater degree of control over the optical properties of the substrate. The alternative confinement geometry for plasmons provided by the nanovoids is less sensitive to nanoscale sharp features (as for example are nanoparticles) enabling controllable and uniform SERS enhancements. In addition, large areas (up to 1.5 cm^2 so far) may be produced with reproducible SERS obtained across the entire area. The nanovoid substrates are robust; reproducible results have been obtained using substrates up to a year after electrodeposition and substrates can be re-used following removal of the adsorbate (by electrochemical oxidation in the case of benzene thiol). The resulting substrates are also inherently electronically conductive, enabling their use in electrochemical SERS measurements.[15]

Fig. 4 shows the effect of increasing the thickness of the film electrodeposited through the template on the structure that remains after the latex spheres are removed. Very thin films may be described as a regular, hexagonal array of circular holes (4a). As the thickness is increased up to 0.5*d* the sculpted substrate corresponds to an array of hemispherical dishes (4b). Beyond 0.5*d* the dishes begin to close over, leaving an array of truncated spherical voids (4c).

The effect of film thickness on the SERS spectra of adsorbed benzene thiol is illustrated by the thickness *vs*. wavenumber image shown in Fig. 5. The spectra were obtained using a graded substrate in which the thickness was increased in steps of 0.08*d* from 0*d* to 0.8*d*. Bright areas of the image correspond to greater SERS intensity. Two peaks in the SERS intensity as a function of film height are observed between 0.3*d* and 0.4*d* and between 0.5*d* and 0.75*d*.

Reflectance spectra were obtained at the same points on the graded substrate at which the SERS were measured. The reflectance spectra and the corresponding optical images of the sample are

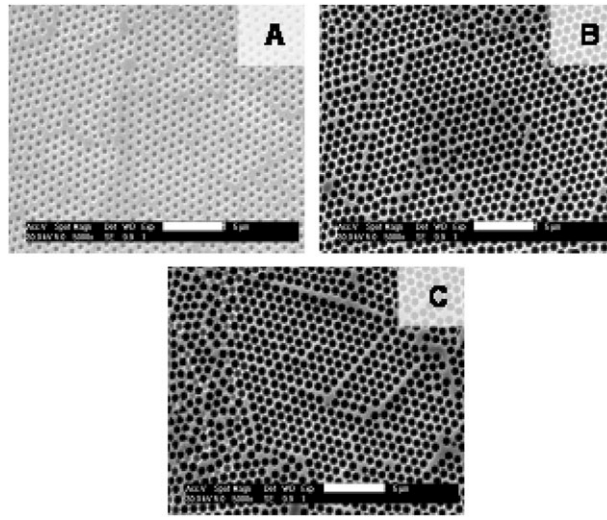

Fig. 4 SEM images of sculpted substrates prepared using $d = 600$ nm spheres, grown to thickness of (a) $0.2d$, (b) $0.5d$, and (c) $0.75d$.

shown in Fig. 6. The features observed in the reflectance spectra will be discussed in detail below, but it is clear that the greatest SERS intensities are obtained at film thicknesses where there is a corresponding increase in the absorbance, and therefore decrease in the reflectance, at approximately 633 nm in the reflectance spectra.

We have recently shown that absorbance features observed in the reflectance spectra of the sculpted surface may be described in terms of the relative contributions of surface plasmon-polaritons (SPP), or Bragg plasmons, and localised Mie plasmons.[20] The former are apparent in the reflectance spectra of the thinner, $\leq 0.5d$ films, and the effects of both are apparent in the reflectance spectra obtained for the thicker films. For the thinnest films, $< 0.2d$ thick, the surface of the metal film consists of a hexagonal array of shallow circular dishes, with the top surface consisting of flat areas of metal separating the dishes. Surface plasmon-polaritons are able to travel across this surface, being scattered off the rims of the dishes, giving rise to Bragg modes. These modes are evident as the absorbance features in the reflectance spectra observed between 550 nm and 600 nm for the thinner films, and they move to shorter wavelengths as the film thickness is increased. At a

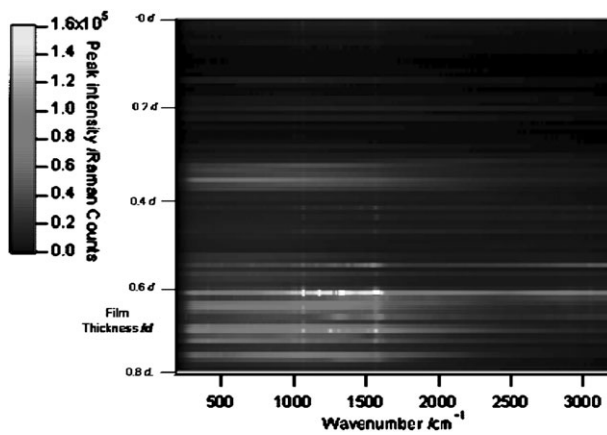

Fig. 5 SERS image of the 1571 cm^{-1} peak of benzene thiol adsorbed onto a graded thickness $d = 600$ nm sculpted surface as a function of the film height. Brighter colours correspond to greater SERS intensity.

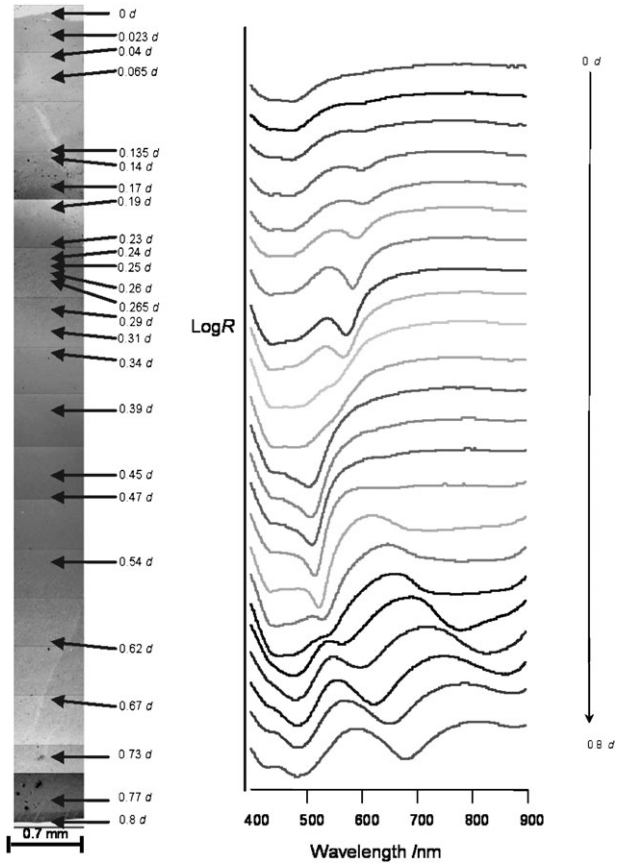

Fig. 6 Optical images (left) and reflectance spectra (right) of the graded $d = 600$ nm sculpted surface used to obtain the Raman image shown in Fig. 5. The reflectance spectra, offset for clarity, were obtained using a white light laser source and are plotted on a log scale. The arrows indicate the points at which the reflectance spectra were obtained.

thickness of $0.5d$, corresponding to hemispherical voids, the top surface breaks up into disconnected triangular islands and the fraction of the area of the top surface that is flat is a minimum. At this point the scattering of the Bragg modes at the top surface is at a maximum. For films with thickness $\geq 0.4d$ localised plasmons are trapped within the spherical cavities in addition to the surface plasmons travelling across the top surface. For fully spherical voids, *i.e.* if the top surface were to close over, these trapped plasmons may be modelled using Mie scattering and, therefore, they have been described as Mie modes. The Mie and Bragg modes interfere with the incoming light and this interference produces the series of absorbance features observed in the reflectance spectra of the thicker films between 475 nm and 700 nm.

Sculpted substrates were prepared using spheres with diameters ranging from 350 nm to 800 nm. The most intense SERS spectra of adsorbed benzene thiol obtained using 633 nm excitation for each of the substrates are shown in Fig. 7 (the film thicknesses are quoted in the figure caption). The greatest SERS intensity was obtained using the 350 nm diameter spheres and the calculated enhancement factor for this surface was 6.6×10^8.

The reflectance spectra as a function of the sphere diameter, corresponding to the SERS data in Fig. 7, are shown in Fig. 8. The wavelengths corresponding to the laser excitation, 633 nm, and Raman scattered photons of the 1571 cm^{-1} SERS peak, 703 nm, are indicated in Fig. 8. As observed above for the surface prepared using 600 nm diameter spheres, the intensity of the SERS peaks, and therefore the enhancement factor, is greatest for those substrates for which the wavelength of the

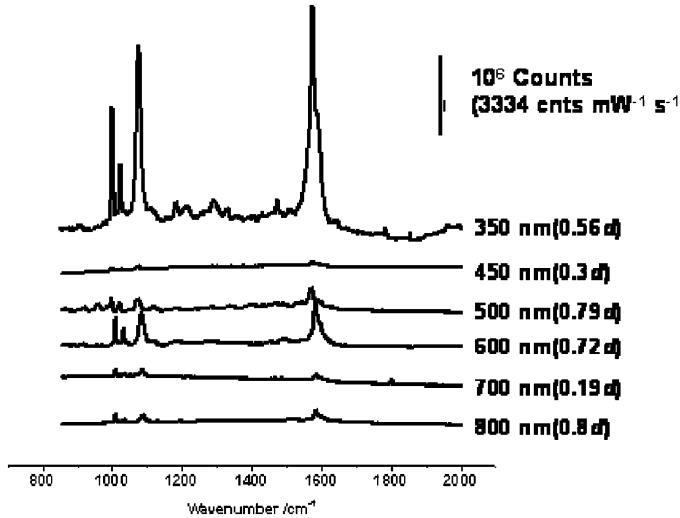

Fig. 7 SERS of benzene thiol adsorbed on sculpted substrates as a function of sphere diameter. Note that the substrates were deposited to various thicknesses as indicated in the diagram. The reported spectra represent the largest SERS enhancements for each sphere size.

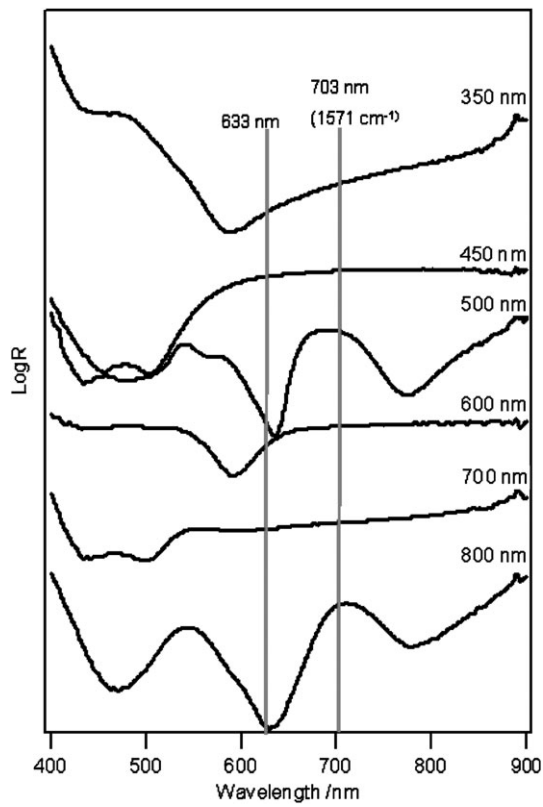

Fig. 8 Reflectance spectra corresponding to the sculpted surfaces used in Fig. 7.

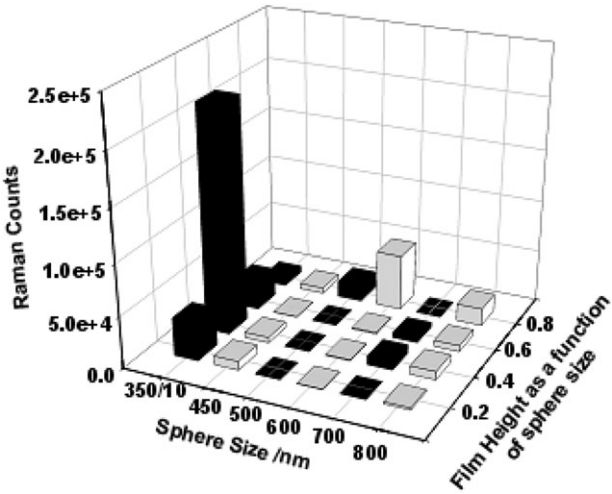

Fig. 9 Peak intensity of the 1571 cm^{-1} band in the SERS spectrum of adsorbed benzene thiol as a function of the sphere diameter, *d*, and fractional film thickness.

excitation laser, 633 nm in this case, overlaps with a strong absorption feature in the reflectance spectra. However, as well as the ingoing resonance at the pump wavelength, we have recently demonstrated the importance of outgoing plasmon resonance at the Raman scattered photon energy.[21] In agreement with this observation, the largest SERS signal (greatest enhancement) was obtained for the 350 nm sample, where absorbance was observed at both the pump and Raman wavelengths. This result implies that it is not possible to produce a completely general SERS enhancement substrate, but that substrates must be matched to the particular excitation wavelength and Raman band used.

The SERS enhancement obtained for our sculpted substrates is dependent on both the sphere (or void) diameter and the film thickness. In a further investigation, using a combinatorial approach, substrates with graded thicknesses were prepared for each sphere diameter investigated and the SERS intensity of the peak at 1571 cm^{-1} for adsorbed benzene thiol, corresponding to the ring breathing mode, is plotted as a function of sphere diameter and fractional thickness in Fig. 9.

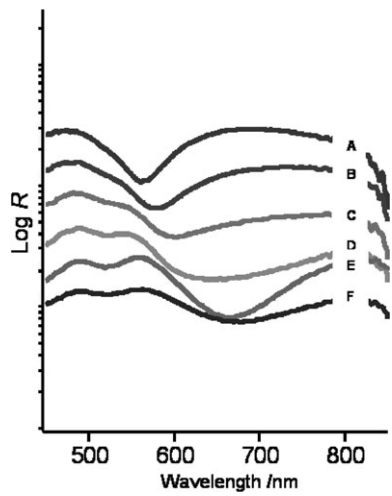

Fig. 10 Reflectance spectra obtained for the 350 nm diameter sculpted surface as a function of film thickness. Spectra are shown for film thicknesses of (a) 0.2*d*, (b) 0.35*d*, (c) 0.5*d*, (d) 0.6*d*, (e) 0.7*d*, and (f) 0.8*d*.

By far the greatest SERS intensity is observed for the sculpted substrates prepared using the 350 nm spheres. The reflectance spectra as a function of film thickness for this substrate are shown in Fig. 10. In contrast to the spectra obtained using the 600 nm surface shown in Fig. 6, the absorbance features in the spectra of the 350 nm surface are broad at all thicknesses and are attributed to localised plasmon modes. The top surface of sculpted substrates prepared using such small spheres have smaller flat areas and SPP are unable to propagate far without scattering off the other features of the surface. The absorbance features attributed to such SPP modes are, therefore, expected at wavelengths below the 400 nm cut-off of the reflectance spectra.

Conclusions

The sculpted nanovoid substrates described here have enabled the systematic study of the role of localised surface plasmons with defined modes in determining the enhancement factor obtained in SERS measurements. Control over two parameters, void diameter (sphere size) and film thickness (as fraction of void diameter), has provided access to a larger parameter space than previously possible using nanoparticle assemblies. This greater degree of control has highlighted the effects of plasmon resonances at both the excitation/pump wavelength and Raman scattered wavelength, with the greatest enhancements obtained when localised plasmon resonances are present at both wavelengths. Appropriate choice of the two parameters will enable the design of SERS substrates with optical properties that can be tailored to the laser excitation and adsorbate to provide the greatest enhancement specific to the system of interest.

References

1 M. Fleishmann, P. J. Hendra and A. J. McQuillan, *Chem. Phys. Lett*., 1974, **16**, 163.
2 D. L. Jeanmarie and R. P. Van Duyne, *J. Electroanal. Chem*., 1977, **84**, 1.
3 M. G. Albrecht and J. A. Creighton, *J. Am. Chem. Soc*., 1977, **99**, 5215.
4 M. Moskovits, *Rev. Mod. Phys*., 1985, **57**, 783.
5 P. Kambhampati, C. M. Child, M. C. Foster and A. Campion, *J. Chem. Phys*., 1998, **108**, 5013.
6 G. C. Shatz and R. P. Van Duyne, in *Electromagnetic Mechanism of Surface Enhanced Spectroscopy*, ed. J. M. Chalmers and P. R. Griffiths, John Wiley and Sons Ltd., Chichester, 2002.
7 R. C. Maher, L. F. Cohen, P. Etchegoin, H. J. N. Hartigan, R. J. C. Brown and M. J. T. Millington, *J. Chem. Phys*., 2004, **120**, 11746.
8 A. M. Michaels, J. Jiang and L. Brus, *J. Phys. Chem. B*, 2000, **104**, 11965.
9 K. Kneipp, Y. Wang, H. Kneipp, I. Itzkan, R. R. Dassari and M. S. Feld, *Phys. Rev. Lett*., 1996, **76**, 2444.
10 C. L. Haynes and R. P. Van Duyne, *J. Phys. Chem. B*, 2003, **107**, 7426.
11 J. B. Jackson and N. J. Halas, *Proc. Natl. Acad. Sci*., 2004, **101**, 17930.
12 J. Aizpurua, P. Hanarp, D. S. Sutherland, M. Kall, G. W. Bryant and F. J. G. de Abajo, *Phys. Rev. Lett*., 2003, **90**, 57401.
13 S. J. Oldenberg, R. D. Averitt, S. L. Westcott and N. J. Halas, *Chem. Phys. Lett*., 1998, **288**, 243.
14 P. M. Tessier, O. D. Velev, A. T. Kalambur, J. F. Rabolt, A. M. Lenhoff and E. W. Kaler, *J. Am. Chem. Soc*., 2000, **122**, 9554.
15 M. E. Abdelsalam, P. N. Bartlett, J. Baumberg, T. Kelf, S. Cintra and A. E. Russell, *Electrochem. Commun*., 2005, in press.
16 P. N. Bartlett, P. R. Birkin and M. A. Gahanem, *J. Chem. Soc., Chem. Commun*., 2000, **2000**, 1671.
17 P. N. Bartlett, J. J. Baumberg, S. Coyle and M. Abdelsalam, *Faraday Disc*., 2003, **123**, 19.
18 Z. Q. Tian, B. Ren and D. Y. Wu, *J. Phys. Chem. B*, 2002, **106**, 9463.
19 M. E. Abdelsalam, P. N. Bartlett, J. J. Baumberg, T. Kelf, S. Cintra and A. E. Russell, *Phys. Chem. Chem. Phys*., submitted.
20 T. A. Kelf, Y. Sugawara, J. J. Baumberg, M. Abdelsalam and P. N. Bartlett, *Phys. Rev. Lett*, submitted.
21 J. J. Baumberg, T. A. Kelf, Y. Sugawara, S. Cintra, M. E. Abdelsalam, P. N. Bartlett and A. E. Russell, *Nat. Mater*., submitted.